

The use of the Long Baseline Array in Australia for precise geodesy and absolute astrometry

Leonid Petrov · Chris Phillips · Alessandra Bertarini · Adam Deller ·
Sergei Pogrebenko · Ari Mujunen

the date of receipt and acceptance should be inserted later

Received: tbd / Accepted: tbd

Abstract We report the results of a successful 12 hour 22 GHz VLBI experiment using a heterogeneous network that includes radio telescopes of the Long Baseline Array (LBA) in Australia and several VLBI stations that regularly observe in geodetic VLBI campaigns. We have determined positions of three VLBI stations, ATCA-104, CEDUNA and MOPRA, with an accuracy of 3–30 mm using a novel technique of data analysis. These stations have never before participated in geodetic experiments. We observed 105 radio sources, and amongst them 5 objects which have not previously been observed with VLBI. We have determined positions of these new sources with the accuracy of 2–6 mas. We make conclusion that the LBA network is capable of conducting absolute astrometry VLBI surveys with accuracy better than 5 mas.

Keywords VLBI · coordinate systems

Leonid Petrov
SP Systems, Inc./NASA GSFC, Code 660.1, Greenbelt, MD
20771 USA E-mail: Leonid.Petrov@lpetrov.net

Chris Phillips
Australia Telescope National Facility

Alessandra Bertarini
Institute of Geodesy and Geoinformation, Nussallee 17, Bonn

Adam Deller
Centre for Astrophysics and Supercomputing Swinburne University,
Hawthorn VIC 3123, Australia

Sergei Pogrebenko
Joint Institute for Very Long Baseline Interferometry in Europe

Ari Mujunen
Metsähovi Radio Observatory, Helsinki University of Technology
TKK, Finland

1 Introduction

The method of very long baseline interferometry (VLBI) first proposed by Matveenko et al. (1965) is widely used for geodesy and absolute astrometry. The first dedicated geodetic experiment on January 11, 1969 provided results with 1 meter accuracy (Hinteregger et al. 1972). In the following decades VLBI technology has flourished, sensitivities and accuracies have improved by several orders of magnitude and arrays of dedicated antennas have been built. Nowadays, a network of ~ 30 stations spread over the globe participates regularly in observing programs for the Earth orientation parameters (EOP) monitoring, determination of source coordinates, deriving site positions, and monitoring their changes. These activities are coordinated by the International VLBI Services for Astrometry and Geodesy (IVS) (Schlüter and Behrend 2007).

However, the station distribution over the globe is non-uniform. The majority of radio telescopes are located in the northern hemisphere. This non-uniformity results in a disparity in the density of source catalogues: the number of sources with positions determined at a milliarcsecond level of accuracy in the declination zone $[-90^\circ, -50^\circ]$ is a factor of 5 less than in the zone $[+50^\circ, +90^\circ]$. Disparity in station distribution also results in the appearance of systematic errors in the EOP time series derived from analysis of VLBI observations at this network. Therefore, an increase of the number of observing stations in the southern hemisphere that are able to participate in VLBI observing campaigns under geodesy, absolute astrometry, and space navigation programs is very important.

There are seven radio telescopes in Australia that have VLBI recording equipment: HOBART26, PARKES, TIDBIN64, DSS45, ATCA, CEDUNA, MOPRA, and they po-

tentially can participate in VLBI observing campaigns for astrometry and geodesy. The first four stations are equipped with Mark-4/Mark-5 data acquisition system and they have participated in many IVS observing programs. The last three stations have the Long Baseline Array Data Recorder (LBADR) data acquisition system that is not directly compatible with Mark-4/Mark-5 and they have never before participated in experiments for geodesy and absolute astrometry. Using all stations together is a challenging problem.

The possibility to use sensitive antennas ATCA, CEDUNA, MOPRA for space navigation and astrometry would significantly boost our capabilities to observe objects in the southern hemisphere. On January 14, 2005, stations ATCA-104, CEDUNA, MOPRA and PARKES joined the global VLBI network in the Huygens probe tracking observations during its descent in the atmosphere of Titan (Pogrebenko et al. 2004; Witasse et al. 2006). Detection of the Huygens probe signal on the North America–Australia baselines was crucial for the reconstruction of the probe trajectory with ~ 1 km accuracy at Saturn’s distance of 1.3 billion km, although the uncertainty of the LBA station a priori positions introduced systematic errors in the probe’s positioning. A better a posteriori determination of the site coordinates was required to improve the accuracy of the probe’s trajectory reconstruction.

The Long Baseline Array incorporates 5 main antenna: the PARKES 64 m, the Australia Telescope Compact Array (ATCA) which consists of six 22 m antenna run as a phased array for VLBI, the MOPRA 22 m, the HOBART 26 m and the CEDUNA 30 m. Antennas from the NASA’s Deep Space Network at the Canberra Deep Space Communication Complex, TIDBIN64 and DSS45, regularly join the array as does the HARTRAO 26 m dish in South Africa. The array is used for source imaging, differential astrometry and other applications.

Imaging weak target sources and precise differential astrometry require a catalogue of compact calibrators with the density at least one object within a circle of $2\text{--}3^\circ$ of any direction. A catalogue of such calibrators was created from analysis of the VLBA Calibrator Survey observing campaign (Beasley et al. 2002; Fomalont et al. 2003; Petrov et al. 2005, 2006, 2008a; Kovalev et al. 2007). However, the VLBA cannot see objects with declinations below -50° . The extension of the Calibrator Survey to the southern hemisphere should be derived from analysis of dedicated LBA observing campaigns.

For investigating the possibility of using the LBA antennas for precise geodesy and absolute astrometry we ran two observing sessions: a 1.5 hour long test VLBI experiment and a 12 hour geodetic VLBI experiment.

The goal of these experiments was 1) to determine positions of ATCA, CEDUNA, MOPRA with the position accuracy 1–5 cm; 2) to evaluate the feasibility of running absolute astrometry observing campaigns with the heterogeneous LBA network.

In this paper we present results of these experiments. In Section 2 we describe the experiments, scheduling strategies and the hardware configuration. In Section 3 we describe the way how the heterogeneous data were transformed to the same format, transmitted to the correlator and correlated. In Section 4 we describe the algorithm for data analysis and present our results. Concluding remarks are given in section 5.

2 Observations

On May 16, 2006, stations ATCA-104, CEDUNA, MOPRA, HOBART26, PARKES ran a 1.5 hour long fringe test experiment at 22 GHz. The purpose of the fringe experiment was to test the data path, to test the frequency selection, to detect fringes, and to test data analysis procedure. Stations ATCA-104, CEDUNA, MOPRA recorded with the LBADR system. Data from these stations were converted into Mark-4 format using software developed at Metsähovi for the Huygens VLBI experiment, then the data were test-correlated at the Joint Institute of VLBI in Europe, Dwingeloo (JIVE) and finally correlated at the Bonn correlator. Fringes were found at all baselines, except baselines with CEDUNA. Results from this test run allowed us to determine coarse positions of ATCA-104 and MOPRA, which helped to improve noticeably the Huygens VLBI trajectory reconstruction and encouraged us to run to a full-scale 22 GHz LBA experiment in the geodetic mode.

The telescopes ATCA-104, CEDUNA, HOBART26, MOPRA, PARKES, and SESHAN25 (Figure 1) took part in the 12 hour experiment on June 24, 2007. Only one antenna of the 6-element ATCA array participated in the experiment. Antennas of the ATCA array can move along railroad tracks and can be positioned with 10 mm accuracy at one of 44 fixed stations within 6 km range. The ATCA antenna that was used in the observations was positioned at the station W104, and it is referred to as ATCA-104.

This experiment was very different from routine geodetic VLBI experiments.

- We chose to observe at the K band (22 GHz). Traditionally, geodetic experiments are made in a dual-band mode when emission at S band (2.3 GHz) and X band (8.4 GHz) is recorded simultaneously. The linear combination of delays at the X and S bands is almost entirely free from the contribution of the

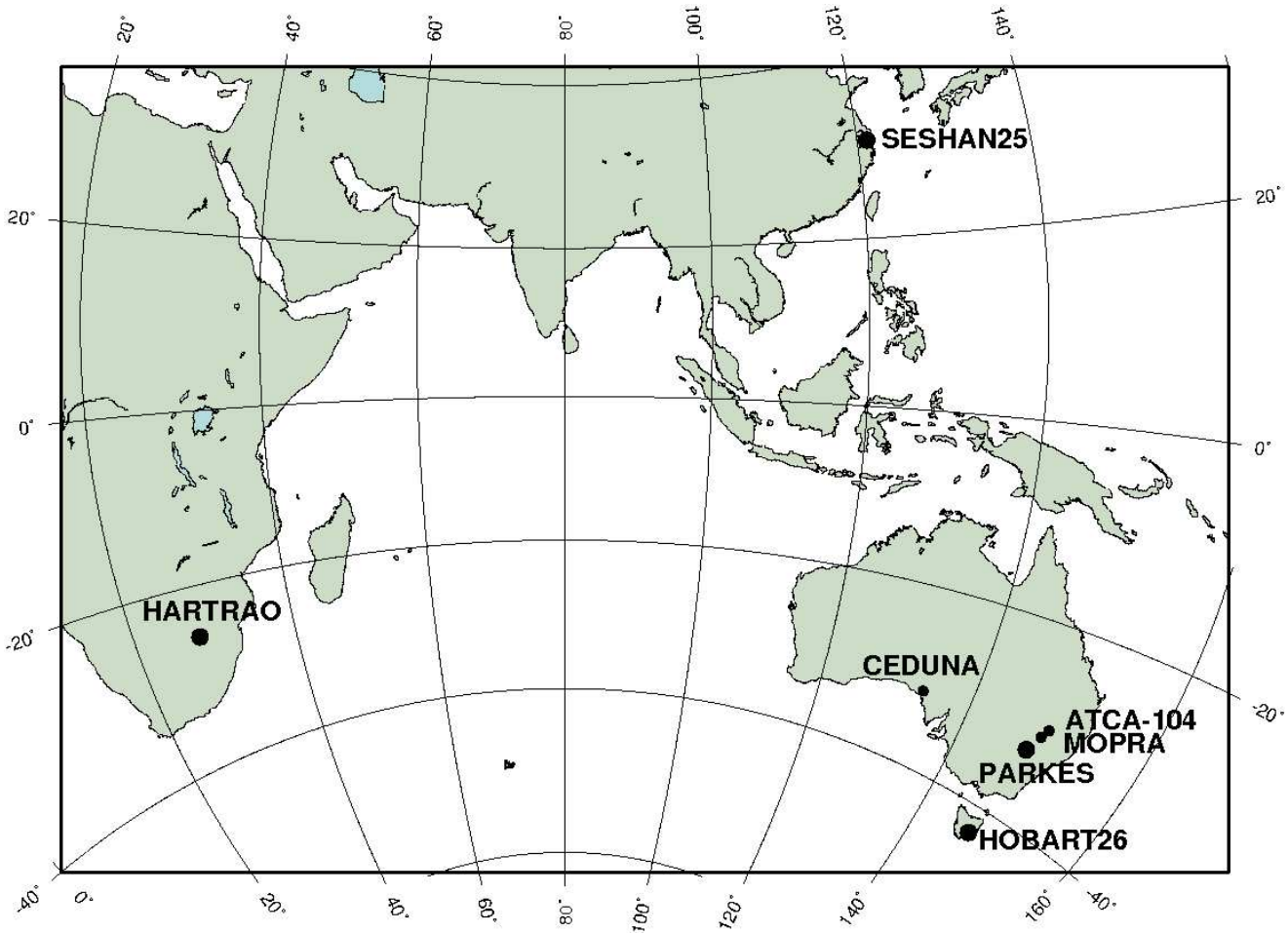


Fig. 1 The network of VLBI stations that participated in the experiment on June 24, 2007. Stations with coordinates known from analysis of prior experiments are shown with big disks.

ionosphere. The antennas ATCA-104, CEDUNA, MOPRA do not have dual-band S/X receivers, so we are limited by only one band. The highest frequency band that all antennas can receive is 22 GHz. Since the ionosphere contribution to group delay is reciprocal to the square of frequency, the ionosphere contribution at the K band is one order of magnitude smaller than the contribution at the X band. Our analysis of K band astrometry observations with the VLBA and several K band geodetic experiments with the VERA showed that the ionospheric contribution at this frequency during the period of low solar activity is negligible, and the overall quality of geodetic results turned out even better than of dual band S/X observations.

- The digital backend used at ATCA, MOPRA and PARKES allows recording of only four pairs of adjacent 16 MHz intermediate frequency channels (IF). CEDUNA can record only two pairs of adjacent IFs. Although the IFs are recorded independently, the system effec-

tively records emission from four channels and always records dual polarization (except CEDUNA), effectively giving only two 32 MHz channels at different frequencies at each polarization. This differs significantly from other VLBI backends such as the Mark-4/Mark-5 and K5 systems which support up to 32 frequency channels and the VLBA recording system which supports up to 8 frequency channels. Traditionally, from 4 to channels per band are allocated. The frequency sequence is selected to minimize the power of sidelobes at the delay resolution function and for avoiding possible radio interferences. No geodetic experiments have ever been made with only two channels.

The frequency sequence that we have chosen for this experiment is shown in Table 1. The frequency difference between two effective 32 MHz channels is 224 MHz. Since the accuracy of group delay determination observed at two effective intermediate frequency channels is reciprocal to the frequency separa-

ration, the wider the frequency separation, the better. From the other hand, the wider the separation of two effective IFs, the smaller group delay ambiguity spacing that is also reciprocal to the frequency separation. The group delay ambiguity spacing in traditional VLBI experiments ranges from 28.5 ns to 200 ns. The spacings were 4.5 ns in our experiment! The a priori model allows to predict path delay with a typical accuracy 3–10 ns, therefore traditional methods of data analysis that use group delays would fail.

Table 1 The range of sky frequencies in the observing session of 2007.06.24, in GHz.

FC1	22.300 — 22.316
FC2	22.316 — 22.332
FC3	22.524 — 22.540
FC4	22.540 — 22.556

- All stations, except CEDUNA, recorded both right circular polarization (RCP) and left circular polarization (LCP). Traditionally, only the RCP is recorded in geodetic experiments. Since the thermal noise of RCP and LCP data is independent, the use of LCP data reduces random errors of parameter estimates.
- The experiment had a heterogeneous setup. Data were recorded at 512 Mb/s, 2 bit sampling, 16 MHz bandwidth per IF, 8 IFs, dual circular polarization (except from CEDUNA that can recorded only RCP). HOBART26, HARTRAO and SESHAN25 used a Mark-4 data acquisition terminals with the setup shown above and wrote data onto disks using the Mark-5a VLBI recorder (Whitney 2005). The rest of the antennas used digital data acquisition system and the LBADR VLBI recorder¹ which is a derivative of the PCEVN² (Parsley et al. 2003). Data were recorded as 16 parallel bit streams. The LBADR uses different physical media for recording than the Mark-5a.

The LBADR system uses the VLBI Standard Interface (VSI-H) (Alan Whitney (2000), unpublished internal document³) signaling and connector conventions. Output bit streams from the VLBI digital backend are converted to the VSI-H using the universal VSI converter board called “VSIC” and captured into regular files on a server-grade PC run under Linux with a VSI-H-to-PCI record board called “VSIB”. To ensure sufficiently high data record rates, Linux software “raid0”

disk sets were used to store the recorded files. This is different from Mark-5 which uses proprietary disk modules as its physical media for recording.

To achieve compatibility with the correlator Mark-5 playback systems, two software solutions were used. The LBADR data of the first 1.5 hour fringe test run were software transformed to Mark-4 format, maintaining timecode information, using custom software running on a computer at JIVE. The resulting files were transferred to a Mark-5a unit to record disk modules for the Bonn correlator.

For the subsequent 12 hour run, software was developed that converts on-the-fly the raw LBADR data to Mark-5b format then sends the data using a tuned TCP stack over the network directly to files residing on a data server at JIVE. Mark-5b compatible disk modules were created and shipped from JIVE to Bonn for correlation. For future such experiments, the LBADR system will write Mark-5b data format directly, but will still not write directly to Mark-5 diskpacs.

2.1 Scheduling

The input list for automatic scheduling consists of 129 compact radio sources. This list was generated by merging two lists for different declination bands. Sources in the declination band $[-30^\circ, +40^\circ]$ were selected from the catalogue of the 252 objects observed at K and Q band with the VLBA in 2002–2006 in the framework of the K/Q astrometric survey (Fey et al. 2005; Jacobs et al. 2005). They have the median K band correlated flux density > 0.4 Jy at baselines longer than 5000 km. Sources in the declination band $[-90^\circ, -30^\circ]$ were taken from the list of sources that were a) observed in geodetic VLBI experiments, b) observed and successfully imaged in astronomy experiments (Ojha et al. 2004), and c) have the median X band correlated flux density > 0.4 Jy at baselines longer than 5000 km.

Automatic scheduling was made with the program SKED developed at the NASA GSFC by N. Vandenberg and J. Gipson (Petrov et al. 2008b). The algorithm for automatic scheduling generated a sequence of scans, i.e. intervals of time of 120 s duration when all antennas of the array, or a portion of the array, are pointed to a specific source and record the emission. Since the list of sources has 129 objects, there exists a very large number of possible sequences. SKED selected the sequence that optimizes the sky coverage at each individual station and minimizes the slew time needed for re-pointing antennas at the next source of the sequence. At each step of generating the sequence of scans, the software finds the distance of a candidate source from all previous sources scheduled within one hour. The candidate

¹ <http://www.atnf.csiro.au/vlbi/>

² <http://www.metsahovi.fi/en/vlbi/boards/index>

³ <http://www.haystack.edu/tech/vlbi/vsi>

source with the largest minimum distance from all previous sources gets the highest sky-coverage score. SKED computes the slewing time and assigns weights to all candidate sources according to their scores based on sky-coverage, slewing time and some other optimization criteria. The source with the highest weight is put into the schedule. The scheduling algorithm adjusts weights to low elevation sources in such a way that each station observes at least one low elevation source every hour. The elevation cutoff was 12° for all the stations, except PARKES, that cannot slew lower than 31° above the horizon.

SKED automatically selected 100 sources. In addition to them, five bright flat-spectrum sources from the Parkes Quarter-Jansky catalogue (Jackson et al. 2002) were inserted in the schedule manually at stations ATCA-104, CEDUNA, MOPRA, HOBART25, PARKES, two scans each. These sources have declination below -55° and have never been before observed with VLBI. The goal of including these sources in the schedule is to evaluate the feasibility of using the LBA for a search of new compact radio sources that can be used as calibrators for phase referencing observations.

3 Data transmission and correlation

Because of the media incompatibility of the LBADR and the Mark-5 format, as well as for convenience, data were transmitted using high speed networks between Australia and Europe. The data transmission was performed directly from the recorder PCs at the observatories in Australia, to a PC located at the JIVE. This was to utilize a dedicated 1 Gbps network which had previously been set up for eVLBI demonstrations as a part of the Express Production Real-time e-VLBI Service. The transmission was made using custom software which uses the TCP network protocol and has been tuned to efficiently use long, wide bandwidth networks. This software also performed an on-the-fly conversion of the LBADR data format to Mark-5b. This simply requires removing the LBADR headers and replacing them with Mark-5b headers (retaining time stamps) as the baseband bit format can be processed by Mark-4 correlators.

After transmission, the Mark-5b data were copied from the PC at JIVE to a Mark-5 disk-pack and shipped to Bonn correlator. Fringe checking was run on the EVN Mark-4 data processor at JIVE before the disk-packs were shipped to Bonn for final correlation. Those station that recorded with the Mark-5a data acquisition system shipped the diskpacks with data to the correlator directly using air mail.

3.1 Correlation

The experiment was correlated at Bonn since the Bonn correlator has previously been thoroughly tested for astrometric and geodetic applications.

The Mark-4 correlator (Whitney et al. 2004) was configured to produce 512 lags and a 0.5 s accumulation period, to have as wide as possible delay and delay-rate fringe search window to allow for possible large station coordinate errors and source position errors. For comparison, the routine geodetic experiments use only 32 lags and accumulation periods of between 2 and 4 s since the errors in the a priori station and source positions are small. In this configuration, the correlator computing capacity is sufficient to process only four stations. Thus, we correlated six passes to form all the baselines between the seven antennas (with some redundancy). The selection of stations for correlation in each pass was guided only by the number of available Mark-5a and Mark-5b units at Bonn, but paying attention not to transpose data from the same antenna when correlating redundant baselines.

Since the LBA stations were not controlled by the Mark-4 field system software and therefore, they did not produce the observation log file required for correlation. Instead, the information required for the correlator control files, such as the scan name and scan times were recovered by comparing information from the Mark-5 module to the schedule file.

A trial correlation was performed to check the correctness of the correlator control files, for example clock offsets, frequencies, polarizations and track assignments. Quality control checks after the each pass were made using the Haystack observatory post-processing system (HOPS) software package.

The stations did not inject phase calibration tones, so phase self calibration was applied to all stations in order to remove IF-dependent phase offsets at those stations with analogue data acquisition terminal (HOBART26, HARTRAO, and SESHAN25). In the 17% of cases where the source was not detected on a baseline, those scans were re-correlated to ensure that these non-detections were not correlator artifacts.

Finally, the multi-band group delays and delay rates were adjusted using the fringe fitting algorithm implemented in HOPS program Fourfit in such a way, that applying these corrections to group delay and delay rate would maximized fringe amplitudes over each scan at each baseline independently.

4 Data analysis

The fringe fit algorithm provides the estimates of fringe amplitudes, fringe phases, phase delay rate, narrow-band group delays, and multi-band group delays. Analysis of amplitude information provides the estimates of the correlated flux densities of observed sources and the sensitivity of antennas. Analysis of fringe phases and delays allows us to estimate station positions and source coordinates.

4.1 Position analysis

Observed delays τ_o depend on an orientation of the baseline vector and the vector of source position, as well as propagation effects and clock functions. The differences between observed delay τ_o and predicted delay τ_c can be used for the parametric adjustment using the least squares:

$$\sum_i \frac{\partial p_i}{\partial \tau} = \tau_o - \tau_c. \quad (1)$$

The overview of the technique for computing predicted delays can be found in Sovers et al. (1998). We used the software library VTD⁴ for computing the theoretical path delay. The expression for time delay derived by Kopeikin and Schäfer (1999) in the framework of general relativity was used. The displacements caused by the Earth's tides were computed using a rigorous algorithm of Petrov and Ma (2003) with a truncation at a level of 0.05 mm based on the numerical values of the generalized Love numbers presented by Mathews (2001). The displacements caused by ocean loading were computed by convolving the Greens' functions with ocean tide models using the NLOADF algorithm of Agnew (1997). The GOT00 model (Ray 1999) of diurnal and semi-diurnal ocean tides, the NAO99 model (Matsumoto et al. 2000) of ocean zonal tides, the equilibrium model of the pole tide and the tide with period of 18.6 years were used. The atmospheric pressure loading was computed by convolving the Greens' functions with the output of the atmosphere NCEP Reanalysis numerical model (Kalnay et al. 1996). The algorithm of computations is described in full details in Petrov and Boy (2004).

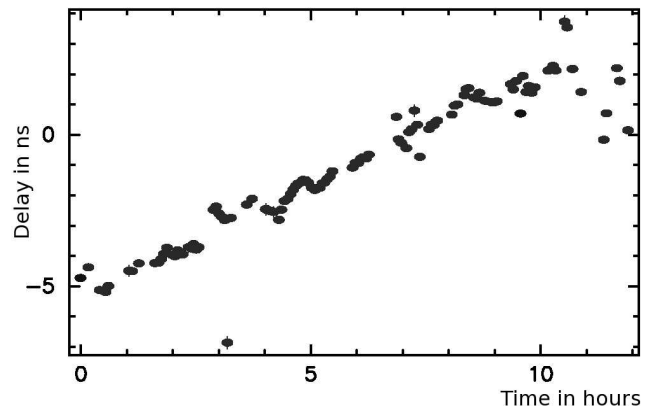
The accuracy of the a priori model is not enough to resolve reliably multi-band group delays computed over the entire recorded bandwidth that have ambiguities

with spacing 4.5 ns. The ambiguity spacing of narrow-band group delays that were computed for each frequency channel separately and then averaged is 16 mks, but the precision or narrow-band delays is worse by the ratio of the width of the entire recorded band to the width of the individual channel, i.e. a factor of 14. The uncertainties of narrow-band group delays are in the range of 0.05–10.0 ns, being below 0.8 ns, i.e. of 1/6 of the multi-band group delay ambiguity spacings for 78% observations. Therefore, a direct substitution of narrow-band delays to multi-band group delays will leave wrong ambiguities for 1/5 of the observations. The time-variable differences between narrow-band delays and multi-band delays due to instrumental effects will worsen the situation even further.

To circumvent the problem, we first made the solution using narrow-band group delays. The estimated parameters were coefficients of the 1st degree B-spline that model clock functions and atmosphere zenith path delay at each station, positions of the three new stations, ATCA-104, MOPRA, CEDUNA, coordinates of five new sources, the pole coordinates and the UT1 angle.

We substituted parameters of the models, adjusted using the narrow-band delays to multi-band group delays. The accuracy of the a priori model with adjustments taken from the narrow-band delay solution turned out sufficient for reliable resolving group delay ambiguities at all baselines. The example of the differences between observed multi-band group delays and predicted are presented in Figures 2–3.

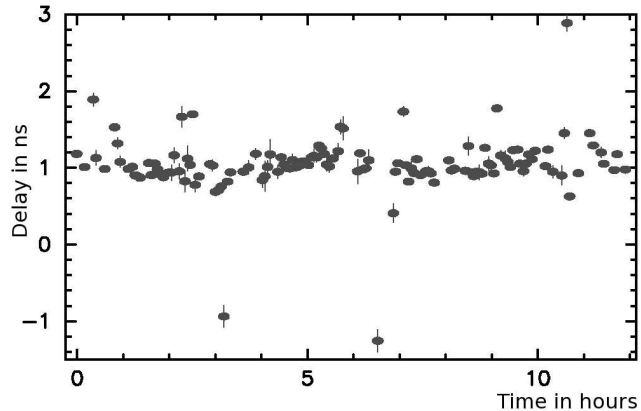
Fig. 2 The differences between observed multi-band group delays and theoretical delays for baseline ATCA-104/CEDUNA predicted on the basis of the a priori model updated with results of the LSQ solution that used narrow-band delays.



During the preliminary fringe test, we used frequencies 23472, 23488, 23600, and 23616 MHz. This frequency setup resulted in ambiguity spacings 7.8125 ns. Analysis of the fringe test showed that multi-band de-

⁴ Source code and detailed documentation is available at <http://vlbi.gsfc.nasa.gov/vtd>

Fig. 3 The differences between observed multi-band group delays and theoretical delays for baseline MOPRA/HOBART26 predicted on the basis of the a priori model updated with results of the LSQ solution that used narrow-band delays.



lay ambiguities can be reliably resolved even with twice smaller ambiguities. The fringe amplitudes were very weak at baselines with HOBART26 and no fringes was detected at baselines with CEDUNA. We found that frequencies 23600–23632 MHz were near the edge of the receiver filter at HOBART26 and beyond the filter at CEDUNA. We have adjusted the frequency setup at the 2007.06.24 experiment. The fringe test allowed us to determine positions of ATCA-104 and MOPRA with $1\text{-}\sigma$ errors ~ 1.6 m for the vertical component and ~ 0.2 m for the horizontal component. We found that the a priori coordinate of ATCA-104 had an error of 80 m, apparently due to a confusion of different pads used by the ATCA array.

After successful resolution of group delay ambiguities the outliers were eliminated, and the additive baseline-dependent corrections to weights was evaluated in a trial solution to make the ratio of the weighted sum of squares of residual to their mathematical expectation to be close to unity. The RCP and LCP data were treated as independent experiments. All analysis procedures, group delay ambiguities resolution, outliers elimination and reweighting were made independently for the LCP and RCP datasets.

Finally, the RCP and LCP data from the 12 hour run were used in a global least square (LSQ) solution together with all available VLBI data, 4431 twenty four hour experiments from 1980 through 2008.

The estimated parameters belong to one of the three groups:

- *global* (over the entire data set): coordinates of 3094 sources, including 5 new sources observed during the experiment on 2007.06.24, positions of 152 stations, including positions of all stations observed on 2007.06.24.

- *local* (over each session): tilts of the local symmetry axis of the atmosphere for all stations and their rates, station-dependent clock functions modeled by second order polynomials, baseline-dependent clock offsets.
- *segmented* (over 0.33–1.0 hours): coefficients of linear spline that models atmospheric path delay (0.33 hour segment) and clock function (1 hour segment) for each station. The estimates of clock function absorb uncalibrated instrumental delays in the data acquisition system.

The rate of change for the atmospheric path delay and clock function between two adjacent segments was constrained to zero with weights reciprocal to $1.1 \cdot 10^{-14}$ and $2 \cdot 10^{-14}$, respectively, in order to stabilize solutions. The weights of observables were computed as $w = 1/\sqrt{\sigma_o^2 + r_b^2}$, where σ_o is the formal uncertainty of group delay estimates and r_b is the additive baseline-dependent reweighting parameter.

Since the wave propagation equations are differential equations, their solution does not determine object coordinates and their derivatives uniquely. As a result, the matrix of normal equations that emerges in solving equations 1 has incomplete rank. In order to overcome the rank deficiency, we impose constraints that require the net-rotation and net-translation of the estimates of positions and velocities of 35 selected sites with respect to positions from the ITRF2005 catalogue (Altimimi et al. 2007) to be zero, and the net-rotation of 212 sources with respect to the ICRF catalogue (Ma et al. 1998) be zero as well.

Results of the solution are shown in Tables 2 and 3⁵. The $1\text{-}\sigma$ uncertainty of the vertical position of ATCA-104 and MOPRA are 12 mm, and the uncertainty of their horizontal position is 4 mm. The $1\text{-}\sigma$ uncertainty of the vertical position of CEDUNA is 28 mm, and the uncertainty of its horizontal position is 6 mm.

All five new sources were detected and their coordinates were determined with the $1\text{-}\sigma$ uncertainty 2–5 mas according to Table 3.

4.2 Correlated flux density estimates

Amplitudes of the cross-correlation function are used for estimation of the correlated flux density of observed sources. System temperature was measured at all stations during the experiment, either before each scan or continuously. The correlated flux density F_{corr} is proportional to the amplitude of the cross correlation A_{corr} :

⁵ A machine readable version of this table is also accessible in the electronic supplement.

Table 2 Position of the three new stations on epoch 2007.06.24. Units: meters.

Station	X	Y	Z
ATCA-104	-4751640.182 ± 0.008	2791700.322 ± 0.006	-3200490.668 ± 0.007
CEDUNA	-3753443.168 ± 0.017	3912709.794 ± 0.017	-3348067.060 ± 0.016
MOPRA	-4682769.444 ± 0.009	2802618.963 ± 0.006	-3291758.864 ± 0.008

Table 3 Coordinates of five new sources at the J2000.0 epoch. The column (u) shows the number of observations used in the solution. The column (s) shows the number of scheduled observations. Units are hours, minutes and seconds for right ascensions; degrees, arc-minutes and arc-seconds for declinations.

Source	α	δ	(u)	(s)
0100-760	01 02 18.6609 ± 0.0018	-75 46 51.730 ± 0.003	24	32
0219-637	02 20 54.1722 ± 0.0004	-63 30 19.387 ± 0.002	31	32
0333-729	03 32 43.0009 ± 0.0011	-72 49 04.521 ± 0.004	18	32
1941-554	19 45 24.2477 ± 0.0007	-55 20 48.949 ± 0.006	5	16
2140-781	21 46 30.0694 ± 0.0003	-77 55 54.735 ± 0.002	25	25

$$F_{corr} = \sqrt{\frac{T_{s1}^* T_{s2}^*}{D_1 D_2}} g_1 g_2 A_{corr}, \quad (2)$$

where T_{s1}^* and T_{s2}^* are system temperatures at stations 1 and stations 2 corrected for the extinction in the atmosphere, D_1 and D_2 are the a priori elevation-dependent antenna gains for both antennas of the baseline, and g_1 , g_2 are empirical a posteriori multiplicative gain corrections.

The a priori gains were obtained from prior dedicated observations of bright sources. Its dependence on elevation was modeled with a polynomial.

Recorded system temperature was considered as a sum of two terms: the receiver temperature T_{rec} and the contribution of the atmosphere:

$$T_{sys} = T_{rec} + T_{atm}[1 - e^{-\alpha m(e)}], \quad (3)$$

where T_{atm} is the average temperature of the atmosphere, α is the atmosphere opacity, and $m(e)$ is the wet mapping function: the ratio of the neutral atmosphere non-hydrostatic path delay at an elevation e to the atmosphere non-hydrostatic path delay in the zenith direction. We omitted in expression 3 the ground spillover term that was not determined for these antennas. We set T_{atm} to 280K, and evaluated the receiver temperature and the opacity factors for each antenna by fitting them into records of system temperatures with the use of the non-linear LSQ. The results are presented in Table 4. The system temperature divided by $e^{-\alpha m(e)}$, T_s^* , is free from absorption in the atmosphere.

The a priori antenna gain D and/or T_{sys} may have a multiplicative error. The corrections to antenna gain were evaluated by fitting the correlated amplitude to the flux density of sources with known brightness distribution. Of 97 sources detected in our experiment, 38

Table 4 Parameters of the radio telescopes determined from the experiment. Column 2 contains the averaged adjusted SEFD at elevation angles $> 60^\circ$. Column 3 contains the multiplicative error factor of the SEFD estimate. Column 4 and 5 contain the estimates of the receiver temperature and the atmosphere opacity in the zenith direction.

Station	SEFD Jy	m.e.f.	T_{rec} K	opacity
ATCA-104	850	0.17	26	0.17
CEDUNA	8300	0.19	164	0.10
HARTRAO	7900	0.37	206	0.06
HOBART26	2300	0.18	144	0.50
MOPRA	890	0.17	26	0.12
PARKES	970	0.25	60	0.06
SESHAN25	10000	0.21	119	0.27

objects were imaged in the VLBA K-band experiment on 2006.07.09 under the K/Q band survey program. brightness distributions of these objects and many others were made publicly available by Alan Fey⁶. We have computed the logarithms of the predicted correlated flux density at moments of observations for these 38 sources considered as amplitude calibrators. We used them for determining logarithms of corrections to gains by the LSQ fit to the logarithms of observed correlated amplitudes according to equation 2. Although the correlated flux density of the calibrators may change for one year between epochs of observations due to image evolution, the large number of calibrators provides rather robust estimates of gain corrections. The estimates of the mean system equivalent flux density, defined as $g T_{sys} e^{\alpha m(e)} / D$ — the parameter that characterizes the sensitivity of a radio telescope, are presented in Table 4 for elevations $[60^\circ, 90^\circ]$. Since the corrections to gains are multiplicative, their errors are characterized by a multiplicative error factor (m.e.f.).

Using gain corrections, we have computed the calibrated flux density for other 59 detected sources. Since

⁶ <http://rorf.usno.navy.mil/rfid.shtml>

we have too few observations of each individual source, we made no attempt to produce images. We have computed the mean correlated flux density in four ranges of the baseline projection lengths: 0–50 megawavelengths, 50–150 megawavelengths, and 400–800 megawavelengths. The results are presented in Table 5. The errors of correlated flux density estimates for point-like sources are determined by errors of amplitude calibration that are the mean m.e.f. from Table 4, i.e. $\sim 20\%$.

5 Conclusions and future observations

The K-band geodetic VLBI experiment with using the LBA network and SESHAN25 turned out highly successful. Position of ATCA-104 and MOPRA were determined with $1\text{-}\sigma$ formal uncertainty 12 mm for the vertical component and 4 mm for the horizontal components. The catalogue of site positions and velocities in our solution does not have net rotation and net translation with respect to the IRTF2005 catalogue, therefore our estimates of site positions are consistent with the ITRF2005. Since relative positions of 44 ATCA stations were previously measured with ground survey, using our coordinates of ATCA-104 we have derived absolute positions of other 43 pads. The table of absolute positions of the ATCA antenna stations can be found at <http://vlbi.gsfc.nasa.gov/lcs/coord>. Position of CEDUNA was determined with the uncertainty 28 mm for the vertical and 6 mm for the horizontal components. Worse position accuracy of CEDUNA is explained by 10 times worse antenna sensitivity and the lack of LCP data.

We have demonstrated that VLBI experiments for absolute astrometry and geodesy at the array with a heterogeneous setup that uses the LBADR and Mark-5 data acquisition systems are feasible and can provide high quality results.

We have demonstrated that the group delay ambiguities with spacings as small as 4.5 ns can be successfully resolved using the adjustments to the a priori model from the narrow-band delay solution.

We have determined positions of 5 new sources never observed before with the VLBI with the $1\text{-}\sigma$ uncertainties of 2–5 mas. This result proves that the LBA can be used for absolute astrometry observations.,

Inspired by these astrometric results, we launched the X-band LBA Calibrator Survey observing campaign⁷ for determining positions and images of thousands of objects with declinations below -50° . The first observing session ran successfully in February 2008.

Table 5 The mean correlated flux density of observed sources in jansky, except amplitude calibrators, at three ranges of the baseline projection length.

Source	# Obs	Correlated flux density in Jy		
		0–50 M λ	50–150 M λ	400–800 M λ
0047–579	23	1.78	0.90	...
0048–097	13	1.12	1.25	...
0048–427	8	0.62	0.36	...
0100–760	6	0.38	0.19	...
0104–408	10	3.74	1.95	...
0107–610	5	0.40	0.36	...
0131–522	17	1.08	0.52	...
0219–637	19	0.39	0.31	...
0230–790	10	0.72	0.49	...
0252–549	6	1.52	0.58	...
0302–623	17	1.85	0.73	...
0306+102	23	1.01	0.90	0.69
0316+162	27	2.12	1.02	0.70
0332–403	3	0.57	0.41	...
0333+321	3	1.11	...	0.43
0333–729	11	0.26	0.24	...
0402–362	13	1.20	0.68	...
0438–436	11	0.69	0.43	...
0446+112	4	0.59	0.85	...
0516–621	6	1.23	0.96	...
0537–441	6	9.24	5.83	...
0552+398	3	2.57	...	0.90
0727–115	1	2.37
0738–674	1	0.24
1057–797	29	2.57	1.69	0.82
1144+402	2	1.18
1144–379	3	...	1.92	1.00
1324+224	2	1.14
1334–127	16	4.99	4.37	4.07
1349–439	3	0.43	0.28	...
1406–076	10	1.00	0.88	0.77
1424–418	10	2.51	2.14	0.87
1511–100	27	1.42	1.14	1.18
1610–771	15	1.36	0.60	...
1619–680	14	0.73	0.39	...
1718–649	7	2.54	1.03	...
1732+389	2	0.71	...	1.03
1741–038	14	4.30	3.03	2.27
1749+096	16	6.48	5.48	3.83
1758–651	18	0.94	0.73	0.45
1815–553	11	0.79	0.48	...
1831–711	9	1.74	0.71	0.46
1925–610	16	0.61	0.22	...
1941–554	4	...	0.20	...
1954–388	16	1.74	1.01	...
1958–179	25	2.62	1.80	1.32
2030–689	24	0.56	0.29	...
2052–474	10	2.78	2.15	0.92
2059–786	10	1.11	0.65	...
2121+053	18	1.25	0.87	0.49
2131–021	23	1.55	1.75	1.52
2140–781	15	1.24	1.06	1.00
2142–758	12	0.40	0.23	...
2145+067	26	5.99	5.16	1.57
2236–572	38	0.86	0.62	...
2326–477	36	1.24	0.75	...
2344–514	22	0.27	0.22	...
2353–686	10	1.00	0.49	...
2355–534	10	2.11	1.05	...

⁷ <http://vlbi.gsfc.nasa.gov/lcs>

Acknowledgements EXPReS is an Integrated Infrastructure Initiative (I3), funded under the European Commission's Sixth Framework Programme (FP6), contract number 026642, from March 2006 through February 2009. We greatly appreciate Alan Fey and Roopesh Ojha who made digital images in FITS format from the surveys publicly available and Robert Campbell for performing the highly non-standard test correlations of LBA data at the JIVE correlator.

References

- Agnew, DC (1997) NLOADF: A program for computing ocean-tide loading, *J Geophys Res*, 102(B3):5109–5110
- Altamimi Z, Collilieux X, Legrand J, Garayt B, & Boucher C, (2007), ITRF2005: A new release of the International Terrestrial Reference Frame based on time series of station positions and Earth Orientation Parameters, *J. Geophys. Res.*, 112, B09401, doi:10.1029/2007JB004949
- Beasley AJ, Gordon D, Peck AB, Petrov L, MacMillan DS, Fomalont EB, Ma C (2002) The VLBA Calibrator Survey—VCS1', *Asrophys J Supp*, 141:13–21, doi:10.1086/339806
- Hinteregger HF, Shapiro II, Robertson DC, Knight CA, Ergas RA, Whitney AA, Rogers AEE, Moran JM, Clark TA, Burke BF (1972) Precision Geodesy via Radio Interferometry, *Science*, 178, 396
- Fey A, Boboltz DA, Charlot P, Fomalont EB., Lanyi GE, Zhang LD (2005) Extending the ICRF to higher radio frequencies: first imaging results, *ASP Conf Ser*, 340, 514
- Fomalont E, Petrov L, McMillan DS, Gordon D, Ma C (2003) The Second VLBA Calibrator Survey: VCS2, *Astron J*, 126(5):2562–2566, doi:10.1086/378712
- Jackson CA, Wall JV, Shaver PA, Kellermann KI, Hook IM, Hawkins MRS, (2002) The Parkes quarter-Jansky flat-spectrum sample. I. Sample selection and source identifications, *Astron & Astrophys*, 386, 97
- Jacobs CS, Lanyi GE, Naudet CJ, Sovers OJ, Zhang LD, Charlot P, Gordon D, Ma C (2005) Extending the ICRF to Higher Radio Frequencies, In *Astrometry at 24 and 43 GHz ASP Conf Ser*, 340, 523
- Kalnay EM, Kanamitsu M, Kistler R, Collins W, Deaven D, Gandin L, Iredell M, Saha S, White G, Woollen J, Zhu Y, Leetma A, Reynolds R, Chelliah M, Ebisuzaki W, Higgins W, Janowiak J, Mo KC, Ropelewski C, Wang J, Jenne R, Joseph D (1996) The NCEP/NCAR 40-Year Reanalysis Project, *Bull Amer Meteorol Soc*, 77:437–471
- Kopeikin SM, Schäfer G (1999) Lorentz covariant theory of light propagation in gravitational fields of arbitrary-moving bodies, *Phys Rev D*, 60(12):124002, doi:10.1103/PhysRevD.60.124002
- Kovalev YY, Petrov L, Fomalont E, Gordon D (2007) The Fifth VLBA Calibrator Survey: VCS5, *Astron J*, 133(4):1236–1242, doi: 10.1086/511157
- Ma C, Arias EF, Eubanks TM, Fey AL, Gontier A-M, Jacobs CS., Sovers OJ, Archinal BA, & Charlot P, (1998), The International Celestial Reference Frame as Realized by Very Long Baseline Interferometry, *Astron J*, 116:516–546, doi:10.1086/300408
- Mathews PM (2001) Love numbers and gravimetric factors for diurnal tides, *J Geod Soc Japan*, 47(1):231–236
- Matsumoto K, Takanezawa T, Ooe M (2000) Ocean tide models developed by assimilating TOPEX/POSEIDON altimeter data into hydrodynamical model: a global model and a regional model around Japan, *J Oceanography*, 56:567–581
- Matveenko LI, Kardashev NS, & Sholomitsky GB (1965) On an interferometer with very long baseline, *Izvestija Vysshih Uchebnyh Zavedenij, Radiofizika*, 8, 651 (in Russian)
- Ojha R, Fey AL, Johnston KJ, Jauncey DL, Reynolds JE, Tzioumis AK, Quick JFH, Nicolson GD, Ellingsen SP, Dodson RG, & McCulloch PM (2004) VLBI observations of southern hemisphere ICRF sources, *Astron J*, 127(5):3609–3621, doi:10.1086/421001
- Parsley S, Pogrebenko S, Mujunen A, & Ritakari J, (2003) *Pcevn*, In *ASP Conference Series*, Vol. 306. San Francisco, CA: Astronomical Society of the Pacific, 145
- Petrov L, Ma C, (2003), Study of harmonic site position variations determined by VLBI, *J. Geophys. Res*, 108(B4), 2190, doi: 10.1029/2002JB001801
- Petrov L and Boy JP (2004) Study of the atmospheric pressure loading signal in VLBI observations, *J Geophys Res*, 109:B03405, doi:10.1029/2003JB002500
- Petrov L, Kovalev YY, Fomalont E, Gordon D (2005) The Third VLBA Calibrator Survey: VCS3, *Astron J*, 129(2):1163–1170, doi:10.1086/426920
- Petrov L, Kovalev YY, Fomalont E, Gordon D (2006) The Fourth VLBA Calibrator Survey: VCS4, *Astron J*, 131(3):1872–1879, doi:10.1086/499947
- Petrov L, Kovalev YY, Fomalont E, Gordon D (2008) The Sixth VLBA Calibrator Survey: VCS6, *Astron J*, 136(2):580–585, doi:10.1088/0004-6256/136/2/580
- Petrov P, Gordon D, Gipson J, MacMillan D, Ma C, Fomalont E, Walker RC, Carabajal C (2008) Precise geodesy with the Very Long Baseline Array, submitted to *J Geod* <http://arXiv.org/abs/0806.0167>
- Pogrebenko S, Gurvits L, Campbell R, Avruch I, Lebreton J-P, & van't Klooster K (2004) VLBI tracking of the Huygens probe in the atmosphere of Titan, In *Proceedings of the International Workshop Planetary Probe Atmospheric Entry and Descent Trajectory Analysis and Science*, Lisbon, Portugal, October 2003, ESA SP–544
- Ray RD (1999) A global ocean tide model from TOPEX/POSEIDON altimetry: GOT99.2, NASA/TM-1999-209478, Greenbelt USA
- Schlüter W, Behrend D (2007) The international VLBI service for geodesy and astrometry (IVS): current capabilities and future prospects, *J Geod*, 81(4–5):379–387, doi:10.1007/s00190-006-0131-z
- Sovers OJ, Fanelow JL, Jacobs CS (1998) Astrometry and geodesy with radio interferometry: experiments, models, results, *Rev Modern Phys*, 70(4):1393–1454, doi:10.1103/RevModPhys.70.1393
- Whitney AR, Cappallo R, Aldrich W, Anderson B, Bos A, Casse J, Goodman J, Parsley S, Pogrebenko S, Schilizzi R & Smythe D (2004), Mark 4 VLBI Correlator: Architecture and algorithms, *Radio Sci*, 39, RS1007, doi:10.1029/2002RS002820
- Whitney A (2005) Disk-Based VLBI Recording, In: *ASP Conference series*, 306, 12
- Witasse O, Lebreton J-P, Bird MK, Dutta-Roy R, Folkner WM, Preston RA, Asmar SW, Gurvits LI, Pogrebenko SV, Avruch IM, Campbell RM, Bignall HE, Garrett MA, van Langevelde HJ, Parsley SM, Reynolds C, Szomoru A, Reynolds JE, Phillips CJ, Sault RJ, Tzioumis AK, Ghigo F, Langston G, Brisken W, Romney JD, Mujunen A, Ritakari J, Tingay SJ, Dodson RD, van't Klooster CGM, Blancquert T, Coustenis A, Gendron E, (2006) *J Geophys Res* 111, E07S01